

RESEARCH ARTICLE

# Differential accumulation of pelargonidin glycosides in petals at three different developmental stages of the orange-flowered gentian (*Gentiana lutea* L. var. *aurantiaca*)

Gianfranco Diretto<sup>1</sup>✉, Xin Jin<sup>2</sup>✉, Teresa Capell<sup>2</sup>, Changfu Zhu<sup>2,3,\*</sup> , Lourdes Gomez-Gomez<sup>4\*</sup>

**1** Italian National Agency for New Technologies, Energy and Sustainable Development, Casaccia Research Centre, Rome, Italy, **2** Departament de Producció Vegetal i Ciència Forestal, Universitat de Lleida-Agrotecnio Center, Lleida, Spain, **3** School of Life Sciences, Changchun Normal University, Changchun, China, **4** Instituto Botánico, Departamento de Ciencia y Tecnología Agroforestal y Genética, Facultad de Farmacia, Universidad de Castilla-La Mancha, Campus Universitario, Albacete, Spain

✉ These authors contributed equally to this work.

\* [zhu@pvcf.udl.cat](mailto:zhu@pvcf.udl.cat) (CZ); [marialourdes.gomez@uclm.es](mailto:marialourdes.gomez@uclm.es) (LGG)



## OPEN ACCESS

**Citation:** Diretto G, Jin X, Capell T, Zhu C, Gomez-Gomez L (2019) Differential accumulation of pelargonidin glycosides in petals at three different developmental stages of the orange-flowered gentian (*Gentiana lutea* L. var. *aurantiaca*). PLoS ONE 14(2): e0212062. <https://doi.org/10.1371/journal.pone.0212062>

**Editor:** Changjie Xu, Zhejiang University, CHINA

**Received:** November 16, 2018

**Accepted:** January 26, 2019

**Published:** February 11, 2019

**Copyright:** © 2019 Diretto et al. This is an open access article distributed under the terms of the [Creative Commons Attribution License](https://creativecommons.org/licenses/by/4.0/), which permits unrestricted use, distribution, and reproduction in any medium, provided the original author and source are credited.

**Data Availability Statement:** All relevant data are within the manuscript and its Supporting Information files.

**Funding:** This work was supported by the National Natural Science Foundation of China (31270344); MICINN, Spain (BIO2014-54441-P); International Science & Technology Cooperation Project supported by Jilin Provincial Science & Technology Department, China (20190201013JC); PROGRAMA ESTATAL DE INVESTIGACIÓN CIENTÍFICA Y TÉCNICA DE EXCELENCIA, Spain

## Abstract

Corolla color in *Gentiana lutea* L. exhibits a yellow/orange variation. We previously demonstrated that the orange petal color of *G. lutea* L. var. *aurantiaca* is predominantly caused by newly synthesized pelargonidin glycosides that confer a reddish hue to the yellow background color, derived from the carotenoids. However, the anthocyanin molecules of these pelargonidin glycosides are not yet fully identified and characterized. Here, we investigated the regulation, content and type of anthocyanins determining the petal coloration of the orange-flowered *G. lutea* L. var. *aurantiaca*. Anthocyanins from the petals of *G. lutea* L. var. *aurantiaca* were characterized and quantified by HPLC-ESI-MS/MS (High-performance liquid chromatography-electrospray ionization-tandem mass spectrometry) coupled with a diode array detector in flowers at three different stages of development (S1, S3 and S5). Eleven pelargonidin derivatives were identified in the petals of *G. lutea* L. var. *aurantiaca* for the first time, but quantitative and qualitative differences were observed at each developmental stage. The highest levels of these pelargonidin derivatives were reached at the fully open flower stage (S5) where all anthocyanins were detected. In contrast, not all the anthocyanins were detected at the budlet stage (S1) and mature bud stage (S3) and those corresponded to more complex pelargonidin derivatives. The major pelargonidin derivatives found at all the stages were pelargonidin 3-*O*-glucoside, pelargonidin 3,5-*O*-diglucoside and pelargonidin 3-*O*-rutinoside. Furthermore, the expression of *DFR* (*dihydroflavonol 4-reductase*), *ANS* (*anthocyanidin synthase*), *3GT* (*UDP-glucose:flavonoid 3-O-glucosyltransferase*), *5GT* (*UDP-glucose:flavonoid 5-O-glucosyltransferase*) and *5AT* (*anthocyanin 5-aromatic acyltransferase*) genes was analyzed in the petals of three developmental stages, showing that the expression level of *DFR*, *ANS* and *3GT* parallels the accumulation of the pelargonidin glucosides. Overall, this study enhances the knowledge of the biochemical

(BIO2015-71703-REDT, BIO2017-90877-REDT); European Cooperation in Science and Technology (EUROCAROTEN, OC-2015-1-19780). The funders had no role in study design, data collection and analysis, decision to publish, or preparation of the manuscript.

**Competing interests:** The authors have declared that no competing interests exist.

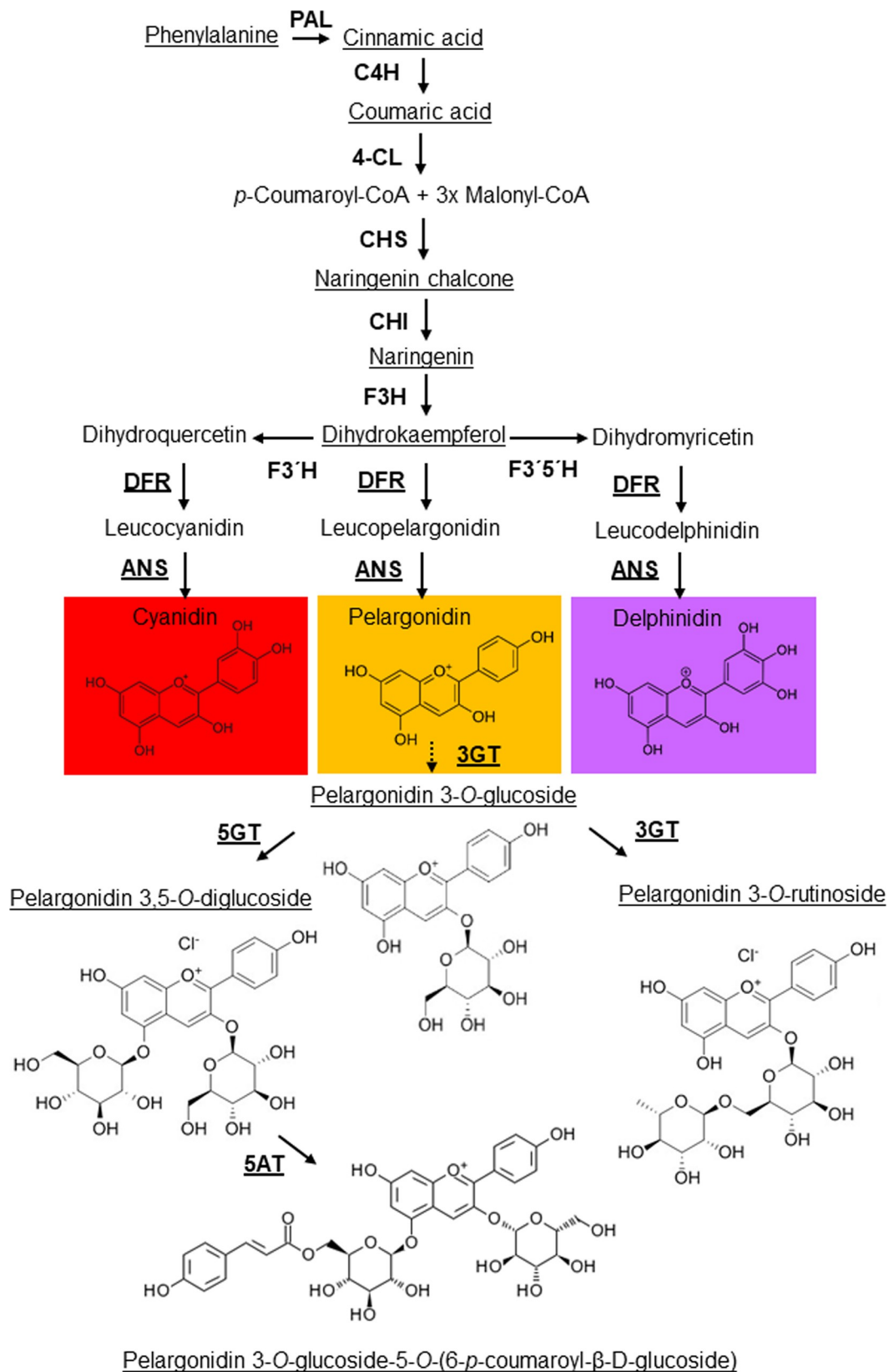
basis of flower coloration in *Gentiana* species, and lays a foundation for breeding of flower color and genetic variation studies on *Gentiana* varieties.

## Introduction

Polymorphism in flower color has been associated with the preferences of pollinators for certain colorations, primarily due to the ability of pollinators to perceive and distinguish among different hues [1–3]. The final color of a flower is determined by the presence of different pigments, mainly carotenoids, flavonoids or betalains [4].

Anthocyanins are water-soluble pigments derived from the flavonoid branch of the phenylpropanoid pathway [5–7]. The genes encoding for enzymes of the anthocyanin pathway are grouped in two classes (Fig 1): early biosynthetic genes, which are common to other flavonoids, encoding enzymes including chalcone synthase (CHS) which is responsible for the formation of naringenin chalcone from 4-coumaroyl CoA and malonyl CoA substrates, chalcone isomerase (CHI) which generates flavones, flavanone 3-hydroxylase (F3H) which produces dihydrokaempferol, flavonoid 3'-hydroxylase (F3'H) and flavonoid 3',5'-hydroxylase (F3'5'H) which generate dihydroquercetin and dihydromyricetin respectively; and late biosynthetic genes, specific to the anthocyanin pathway, encoding enzymes including dihydroflavonol 4-reductase (DFR) and anthocyanidin synthase (ANS) [5–7]. Differences in the hydroxylation of the B-ring of the anthocyanin skeleton confer specific variants in the color range of anthocyanidins: pelargonidins, being orange to red; cyanidins, red to red-purple (by the activity of F3'H); and delphinidins, being red-purple to blue (by the activity of F3'5'H), depending on many other factors [4,7,8]. The resulting anthocyanidin structures are inherently unstable. Therefore, these pigments accumulate exclusively as glycosylated forms, where C<sub>3</sub> is linked through oxygen to a sugar residue, most frequently glucose. UDP-glucose:flavonoid 3-O-glucosyltransferase (3GT) catalyzes the 3-O-glucosylation of anthocyanidins as well as other flavonoids [4]. The generated glycosylated anthocyanins at the 3-position serve as substrates for further modifications such as glycosylation at the 5-position (Fig 1), by the action of UDP-glucose:flavonoid 5-O-glucosyltransferase (5GT) [9,10]. The glycosylation reactions provide sugar residues for decoration with acyl groups by the activity of anthocyanin acyltransferase, which can incorporate aromatic acids such as *p*-coumaric, caffeic, ferulic, sinapic, gallic or *p*-hydroxybenzoic acids, and/or aliphatic acids including malonic, malic, acetic, succinic or oxalic acids. These acyl substituents are commonly bound to the C<sub>3</sub> sugar, esterified to the 6-OH or much less frequently to the 4-OH group of the sugars [11]. Other modification also occurs, such as acylation of the glucose moiety at the 5-position of anthocyanin catalyzed by anthocyanin 5-aromatic acyltransferase (5AT) [12]. Both glucosyltransferases and acyltransferases contribute to the extensive range of natural anthocyanins identified to date, which differ in their side chain decorations, affecting color and increasing pigment stability [6].

The genus *Gentiana* includes over 400 species [13], with a huge range of flower colouration including orange, pink, red, magenta, purple, and blue to blue-black. This color variation is mainly due to the accumulation of anthocyanins and/or carotenoids. Most gentian species of commercial interest in the flower market include those with an intense blue coloration, due to the accumulation of major blue gentiodelphin, a polyacylated delphinidin-type anthocyanin, and minor red gentiocyanin, a cyanidin-derived anthocyanin in petals of *G. triflora* [14,15] and those with pink coloration, associated to the exclusive accumulation of red gentiocyanins in petals of *G. scabra* [16,17]. Both *G. triflora* and *G. scabra* do not accumulate carotenoids in





petals <1.5 cm long with hard bud; stage 3 (S3), mature bud stage, petals 2.5–3.5 cm long with petals slightly loosened; and stage 5 (S5), fully open flower stage.

### Anthocyanin and precursor extraction and identification

All the extractions were performed in triplicate. Freeze-dried petals were ground into a powder and homogeneously ground using 500  $\mu$ L of 85:15 methanol:1 N HCl, and left in the dark at 4°C for 24 h. The extracted liquid was filtered with 0.22  $\mu$ m membrane filter and used for HPLC-DAD analyses as described previously [21].

Anthocyanins were extracted from 10 mg of homogeneously ground petal tissue, using 500  $\mu$ L of 85:15 methanol:1 N HCl with 2  $\mu$ g L<sup>-1</sup> of formononetin (Sigma-Aldrich, USA) as internal standard for quantitative analysis. After shaking for 12 hours and centrifugation for 10 minutes at 15,300 g at 25°C, 0.25 mL of supernatants were transferred to new Eppendorf vials and dried. Samples were then resuspended in 0.1 mL 75% methanol (plus 0.1% formic acid) and centrifuged (10 minutes at 15,300 g at 25°C). Finally, 70  $\mu$ L of supernatants were transferred to HPLC vials for MS (mass spectrometry) analysis, and 5  $\mu$ L of extracts were injected to the HPLC-DAD/MS. HPLC analysis was performed using a C18 Luna column (Phenomenex, Aschaffenburg, Germany) (150  $\times$  2.0 mm; 3  $\mu$ m). 10  $\mu$ L of each extract were injected at a flow of 0.2 mL min<sup>-1</sup>. The mobile phases were: 0.1% formic acid (A) in water and acetonitrile plus 0.1% formic acid (B). The method used for separation was: 95% A: 5% B for 1 min, and a linear gradient to 25% A: 75% B over 40 min, plus an additional 2 min, before returning to the initial conditions for 18 min. Detection was performed continuously from 200 to 600 nm with an online Accela Surveyor photodiode array detector (PDA; Thermo Fisher Scientific). Mass spectrometry analysis was performed using a quadrupole-Orbitrap Q-exactive system (ThermoFisher scientific, USA), as previously described [27] with slight modifications. Metabolite ionization was carried out with a heated electrospray ionization (HESI) source operating in positive ion mode, and nitrogen was used as sheath and auxiliary gas (45 and 15 units, respectively). Mass spectrometer parameters were as follows: capillary and vaporizer temperatures 30°C and 270°C, respectively, discharge current 4.0 KV, probe heater temperature at 370°C, S-lens RF level at 50 V. The acquisition was carried out in the 110/1600 m/z scan range, with the following parameters: resolution 70,000, microscan 1, AGC target 1e6, and maximum injection time 50. A first full scan MS with data-dependent MS/MS fragmentation was used to identify the anthocyanins in the *G. lutea* L. var *aurantiaca* flower extracts. Subsequently, a single ion monitoring (SIM) with targeted MS/MS fragmentation was used to identify anthocyanins for which Data-dependent MS/MS fragmentation was not successful, and to further validate the tentative identifications. Data were analyzed using the Xcalibur 3.1 software (ThermoFisher scientific, USA). Metabolites were identified as M<sup>+</sup> adducts, based on their accurate masses (m/z) and MS fragmentation, using both in house database and public sources (e.g. KEGG, MetaCyc, ChemSpider, PubChem, Metlin, Phenol-Explorer). Relative abundances of the metabolites studied were calculated using the Xcalibur 3.1 software (ThermoFisher scientific, USA). The two most abundant fragments per compound were used to determine the relative abundances, and data were normalized through dividing each peak area by the value of the internal standard peak area [28]. Data are presented as means and standard deviation of at least three independent biological replicates.

For precursor analyses 15 mg of freeze-dried, homogenized *G. lutea* L. var. *aurantiaca* petals were extracted with 0.75 mL cold 75% (v/v) methanol, with 0.1% (v/v) formic acid and spiked with 5  $\mu$ g mL<sup>-1</sup> formononetin. Samples were shaken for 40 min at 20 Hz using a Mixer Mill 300 (Qiagen), before centrifugation for 15 min at 15,300 g. Finally, 0.6 mL of supernatants was placed in the HPLC tubes. HPLC-DAD/MS analyses were carried out using a Q-exactive quadrupole



Orbitrap mass spectrometer (ThermoFisher Scientific), operating in positive/negative heated electrospray ionization (HESI), and coupled to an Ultimate HPLC-DAD system (Thermo Fisher Scientific, Waltham, MA). HPLC conditions were as in the section 4.4. ESI-MS ionization was carried out as follows: sheath and aux gas flow rate set at 40 and 25 units, respectively; vaporizer and capillary temperature were used at 250 and 30°C, discharge current was set at 4.5  $\mu$ A and S-lens RF level at 50. Acquisition was achieved as previously reported. Metabolite identification was carried out using a single ion monitoring (SIM) scan mode, with targeted MS/MS fragmentation, and by comparing chromatographic and spectral properties with authentic standards. Data were analyzed using Xcalibur 3.1 software (ThermoFisher scientific, USA). Metabolites were quantified in a relative way by normalization on the internal standard amounts. Data are presented as means and standard deviation of at least 3 independent biological replicates.

### Cloning of UDP-glucose:Flavonoid 5-O-glucosyltransferase (5GT) and anthocyanin 5-aromatic acyltransferase (5AT) gene fragments from petals of *G. lutea* L. var. *aurantiaca*

Three grams of leaf, petals at S1, S3 and S5 stages, respectively, or mixed petals from S1, S3 and S5 stages (1 g from each stage) were ground into fine powder using mortar and pestle with liquid nitrogen. From these samples, 100 mg samples were used to isolate total RNA for each extraction. Total RNA was isolated using the RNeasy Plant Mini Kit (Qiagen, Valencia, California, USA) and DNA was removed with DNase I (RNase-free DNase Set, Qiagen). The integrity of RNA was confirmed by gel electrophoresis in a denaturing 1.2% (w/v) agarose gel containing formaldehyde. Total RNA was quantified using a Nanodrop 1000 spectrophotometer (Thermo Scientific, Vernon Hills, Illinois, USA), and 1  $\mu$ g total RNA was used as template for first strand cDNA synthesis with QuantiTect Reverse Transcription Kit (Qiagen) in a 20  $\mu$ L total reaction volume, following the manufacturer's recommendations.

A 2  $\mu$ L aliquot of the first strand cDNA product with isolated total RNAs from mixed petals of S1, S3 and S5 stages of *G. lutea* L. var. *aurantiaca* was used in a 50  $\mu$ L RT-PCR reaction containing 1x Green GoTaq Reaction Buffer (Promega, Madison, WI, USA), 0.2 mM of each dNTP, 0.5  $\mu$ M of each primer, and 1.25 U GoTaq DNA Polymerase (Promega, Madison, WI, USA). Reverse transcription polymerase chain reaction (RT-PCR) was performed using primer sequences designed on 5GT and 5AT sequences from *G. triflora*, to amplify partial protein coding sequences of cDNAs for 5GT and 5AT from *G. lutea* L. var. *aurantiaca*. The primer sequences for the 5GT were 5' -CTGCTTCCTTGGGCTGCCGATGTGGCT-3' (forward primer) and 5' -TGCGGATGGAATTCAACGCTGGAGAGC-3' (reverse primer). The primer sequences for the 5AT were 5' -CCGCTCGTAGCCGTGCAAGTAACCGTTTTTCCT-3' (forward primer) and 5' -GATTTTGGATGGGAAAGCCTGCAAATTTGA-3' (reverse primer). The PCR conditions for 5GT and 5AT genes involved heating the reaction to 95°C for 3 min, followed by 35 cycles at 95°C for 45 s, 60°C for 45 s and 72°C for 90 s, and a final extension step at 72°C for 10 min. The resulting expected size products were purified from a 1.0% w/v agarose gel using the GeneClean II Kit (BIO1 101 Systems, Solon, OH, USA) and cloned in pGEM-T easy vector (Promega, Madison, WI, USA) for sequencing with the Big Dye Terminator v3.1 Cycle Sequencing Kit on a 3130x1 Genetic Analyzer (Applied Biosystems, Foster City, CA, USA). Four and six independent clones provided the identical sequences for isolated 5GT and 5AT gene fragments, respectively, from 20 and 26 independent sequenced clones. The nucleotide sequences were translated to the respective deduced amino acid sequences using Vector NTI software, which was also used for alignments of cDNA and deduced amino acid sequences, respectively. Both cloned 5GT and 5AT showed sequence similarity to previously characterized anthocyanin structural genes and BLAST searches against the National Center for

Biotechnology Information (NCBI) nucleotide and protein databases were used to confirm homology with previously characterized *5GT* and *5AT* genes from higher plants [12].

### qRT-PCR analysis of *DFR*, *ANS*, *3GT*, *5GT* and *5AT* expression in leaf, S1, S3 and S5 petals of *G. lutea* L. var. *aurantiaca*

From the above *5GT* and *5AT* partial cDNA sequences, gene-specific primers were designed for these two genes, in order to perform expression analysis by quantitative real-time RT-PCR (qRT-PCR). The primers for the *5GT* were 5′-GCCTTGCAAGCAATCCCAAA-3′ (forward primer) and 5′-CAACCATCCATGGCAGTCCT-3′ (reverse primer). The primers for the *5AT* were 5′-AGCTGTTGGGGATGCCATTG-3′ (forward primer) and 5′-CGATCCACTAATCCCGAGCAA-3′ (reverse primer). Gene-specific oligonucleotides for *DFR*, *ANS*, *3GT* and *UBQ* (ubiquitin gene) were the same as reported previously [21]. Specific primers that amplified a single fragment of no more than 200 bp were designed in regions of the coding sequences isolated from orange-flowered *G. lutea* L. var. *aurantiaca* petals. qRT-PCRs were carried out using a BioRad CFX96 system. Each 25 μL reaction volume comprised 5 ng of cDNA, 1x iQ SYBR green supermix (BioRad, Hercules, CA, USA), and 5 μM of forward and reverse primers. Relative expression levels were calculated on the basis of serial dilutions of cDNA (100–0.16 ng), which were used to generate standard curves for each gene. Triplicate amplifications (biological replicates) were performed in 96-well optical reaction plates by first heating to 95°C for 5 min, followed by 40 cycles at 95°C for 30 s, 58°C for 30 s and 72°C for 30 s. Amplification specificity was confirmed by product melt curve analysis over the temperature range 50–90°C with fluorescence acquired after every 0.5°C increase. The fluorescence threshold value and gene expression data were calculated with BioRad CFX96 software. Data were calculated from three biological replicates with at least three technical replicates for each biological replicate and with error bars representing the standard deviation. Amplification efficiencies were compared by plotting the  $\Delta C_t$  values of different primer combinations of serial dilutions against the log of starting template concentrations using the CFX96 software. The  $C_t$  values were adjusted to the standard curves and normalized against the levels of ubiquitin (*UBQ*) housekeeping gene [21].

### Bioinformatics analyses

Correlation analyses of transcript and metabolite data were performed as previously described [29,30]. Briefly, Pearson correlation coefficients for each data pair (gene-gene, metabolite-metabolite, gene-metabolite) were compiled in Excel and subjected to significance analysis by SPSS software; only correlations showing correlations with P values  $\leq 0.05$  were further processed. Subsequently, correlation matrix was generated using R version 2.10.0, and colored with the Morpheus software (<https://software.broadinstitute.org/morpheus/>). Correlation network analysis was performed using R to generate a network correlation input file, which was finally imported in Cytoscape version 2.6.2 (<http://www.cytoscape.org/>), and visualize using a Prefuse force-directed layout. Node strength (ns) and network strength (NS) were calculated as reported previously [31,32], and represent the average of all the ps (Pearson correlation coefficients) yielded by each node, and the average of all the node strengths in the network, respectively.

## Results and discussion

### Identification of anthocyanins in petals of three developmental stages of *G. lutea* L. var. *aurantiaca*

HPLC reverse phase C18 columns have been extensively used for the separation of anthocyanins in different plant species [33–35]. The acidic methanol extracts of the petals of *G. lutea* L.

var. *aurantiaca* showed mixtures of several peaks (S1 Fig). The anthocyanins corresponding to the peaks (500 nm) observed in the HPLC-DAD chromatogram were characterized and quantified by HPLC-ESI-MS/MS analyses.

All the detected peaks showed a maximum absorbance between 495–505 nm (S1 Fig), characteristic of pelargonidin derivatives [36]. The glycosidic substitution pattern of anthocyanins can be inferred by the presence of absorption in the 400–460 nm region, and the sugar substitution in the 3-OH is deduced by ratio of E440/E<sub>max</sub> about two times greater than those for sugar substitution in both 3- and 5-OH positions [37]. The E440/E<sub>max</sub> ratios obtained for peak 2 was 25% while peak 4 showed a E440/E<sub>max</sub> of 52%, providing evidence that pigment 2 was a 3,5-glycoside and the latter was a 3-glycoside. Identification and peak assignment of anthocyanins was based on the analysis of the mass fragmentation pattern, followed by the comparison of their retention times and mass spectral data with those of standards, if available, and literature data. All the glycosides were tentatively identified using the molecular weight of the aglycone pelargonidin,  $m/z$  271.06008 (Fig 2). In total, eleven major pelargonidin derivatives were identified in the petals at different developmental stages (Table 1). The anthocyanins identified were mainly 3-O-glycoside conjugates and their derivatives. Peak 1 had  $m/z$  of 741.22180 and three mass fragment ions at  $m/z$  579.16992, due to the elimination of one hexose molecule; at  $m/z$  433.11237, indicating the loss of one molecule of rhamnose, and 271.05966, corresponding to pelargonidin (Fig 2G). Therefore, peak 1 was assigned to pelargonidin 3-O-rutinoside-5-O- $\beta$ -D-glucoside (C<sub>33</sub>H<sub>41</sub>O<sub>19</sub>) [38]. Peak 2 (Fig 2E) showed a molecular ion at  $m/z$  595.16516, and two fragment ions of 433.11273 and 271.05972, respectively. Peak 2 was identified as pelargonidin 3,5-O-diglucoside (C<sub>27</sub>H<sub>31</sub>O<sub>15</sub>) [39]. Peak 3 had a molecular ion at  $m/z$  579.17078, and three mass fragment ions, one at  $m/z$  433.11307, due to the elimination of one molecule of rhamnose; one at  $m/z$  271.05981, indicating the loss of rutinoside; and one at 146.05790 for rhamnose. Thus, peak 3 was assigned to pelargonidin 3-O-rutinoside (C<sub>27</sub>H<sub>31</sub>O<sub>14</sub>; Fig 2D). Peak 4 displayed at  $m/z$  433.11203 and a main mass fragment ion at  $m/z$  271.05969, which corresponded to the pelargonidin molecule, due to the elimination of one molecule of glucose (Fig 2A). Therefore, the peak was identified as pelargonidin 3-O-glucoside (C<sub>21</sub>H<sub>21</sub>O<sub>10</sub>; Fig 2A). Peak 5 was characterized by a molecular ion  $m/z$  1094.29358, and four fragment ions:  $m/z$  932.23883, which indicated loss of one hexose;  $m/z$  771.21368, indicative of the loss of caffeoylglucoside;  $m/z$  433.11273, corresponding to pelargonidin and one glucose molecule; and  $m/z$  271.06000, the pelargonidin aglycone. For this reason, peak 5 was designed as pelargonidin 3-O-[2-O-(6-(E)-feruloyl- $\beta$ -D-glucopyranosyl)-6-O-(E)-caffeoyl- $\beta$ -D-glucopyranoside]-5-O-( $\beta$ -D-glucopyranoside) (C<sub>52</sub>H<sub>55</sub>O<sub>26</sub>; Fig 2K). Peak 6 had a molecular ion  $m/z$  1079.30284, and four fragment ions:  $m/z$  932.23871 and  $m/z$  771.21368 indicated the loss of coumaroylglucoside;  $m/z$  771.21368 and  $m/z$  433.11273 indicated the loss of feruloylglucoside, which resulted in pelargonidin glucoside; and  $m/z$  271.05972, corresponding to pelargonidin (Fig 2J). Thus, peak 6 was tentatively assigned to pelargonidin 3-O-[2-O-(6-(E)-feruloyl- $\beta$ -D-glucopyranosyl)-6-O-(E)-*p*-coumaroyl- $\beta$ -D-glucopyranoside]-5-O-( $\beta$ -D-glucopyranoside) (C<sub>52</sub>H<sub>55</sub>O<sub>25</sub>). Peak 7 showed a  $m/z$  843.22095 and five mass fragment ions at  $m/z$  681.16675, due to the loss of a caffeic acid;  $m/z$  595.16333 [M-248.05321 (malonylhexose)];  $m/z$  519.11456 [M-324.08451 (caffeoylhexose)];  $m/z$  433.11392, corresponding to pelargonidin with one glucose; and, finally,  $m/z$  271.06033, the pelargonidin aglycone. This peak (Fig 2I) was tentatively assigned to pelargonidin 3-O-(6-O-caffeoyl-D-glucoside)-5-O-(6-O-malonyl- $\beta$ -D-glucoside) (C<sub>39</sub>H<sub>39</sub>O<sub>21</sub>) [40]. Peak 8 displayed  $m/z$  827.21936, and three mass fragment ions at 579.17004 and 519.11230, which corresponded to the loss of malonylglucoside and coumarylglucoside, respectively; and 271.05972, which represented pelargonidin. Peak 8 was assigned to pelargonidin 3-O-(6-*p*-coumaroyl-D-glucoside)-5-(4-O-malonyl- $\beta$ -D-glucoside) (C<sub>36</sub>H<sub>43</sub>O<sub>22</sub>; Fig 2H). Peak 9 was identified as pelargonidin 3-O-(6-O-malonyl- $\beta$ -D-



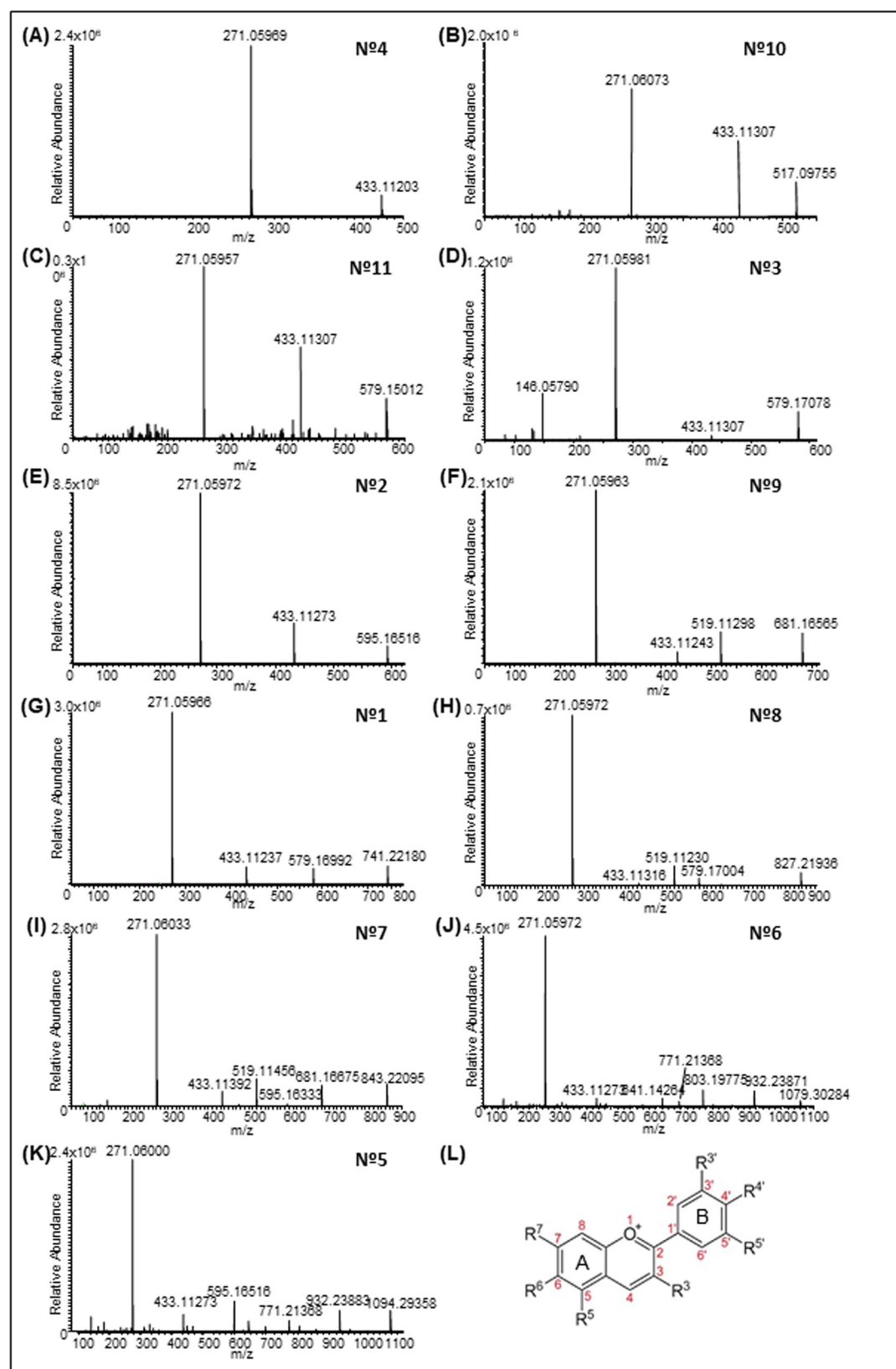


**Fig 2. ESI-MS/MS spectra of anthocyanins isolated from petals of *Gentiana lutea* L. var. *aurantiaca*.** The number from 1 to 11 corresponded with the anthocyanins characterized and listed in Table 1. The image in L corresponded to the basic structure of the anthocyanin molecule.

<https://doi.org/10.1371/journal.pone.0212062.g002>

glucoside)-5-β-D-glucoside (C<sub>30</sub>H<sub>33</sub>O<sub>18</sub>) on the basis of full MS at *m/z* 681.16565 which, upon the loss of a glucose molecule, showed a fragment of *m/z* 519.11298; and the loss of a malonyl-glucoside yielded a fragment at *m/z* 433.11243, corresponding to the pelargonidin unit and a glucose molecule (Fig 2F). Peak 10 and peak 11, finally, showed a molecular ions at *m/z* of 517.09755 and 579.15012, respectively, and were tentatively assigned to pelargonidin 3-*O*-(6-*O*-malonyl-β-D-glucoside) (C<sub>24</sub>H<sub>21</sub>O<sub>13</sub>; Fig 2B) and pelargonidin 3-*O*-(6-*p*-coumaroyl)glucoside (C<sub>30</sub>H<sub>27</sub>O<sub>12</sub>; Fig 2C).

## Quantification of pelargonidin derivatives and precursors in petals at three developmental stages

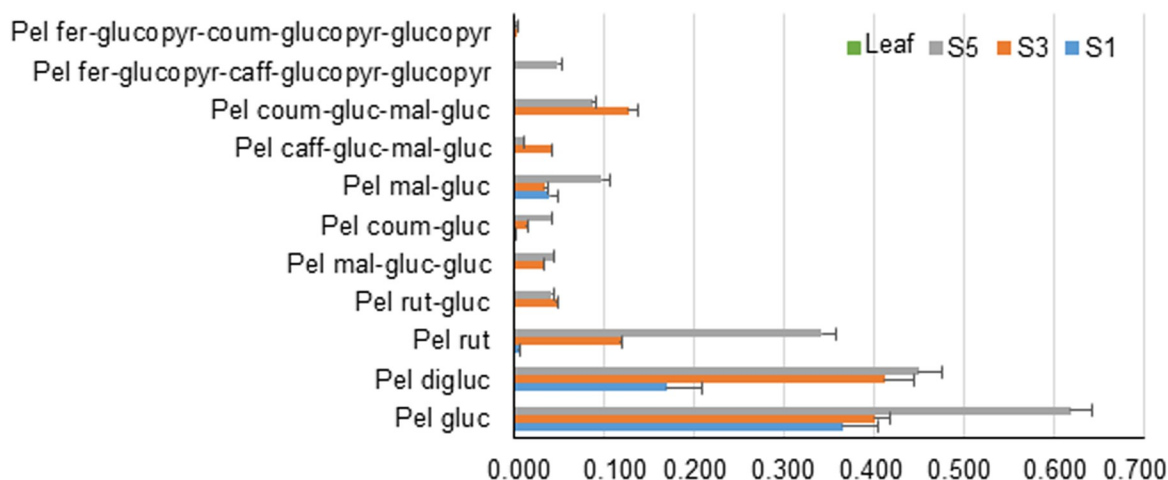
The anthocyanins determined by HPLC-ESI-MS/MS analyses in the petals of *G. lutea* L. var. *aurantiaca* at three developmental stages showed strong variation in abundance (Fig 3). Pelargonidin 3-*O*-glucoside and pelargonidin 3,5-*O*-diglucoside were found to be, by far, the predominant anthocyanins in all the samples analyzed. Interestingly, none of pelargonidin glycosides were detectable in leaves of *G. lutea* L. var. *aurantiaca* (Fig 3). Petals at stage one (S1) were green, and in this stage pelargonidin 3-*O*-glucoside (62.5%) and pelargonidin 3,5-*O*-diglucoside (29.1%) were the main anthocyanins detected (Fig 3 and S2 Fig), followed by far by pelargonidin 3-*O*-(6-*O*-malonyl-β-D-glucoside) (6.8%). Other pelargonidin derivatives

**Table 1. Identification of anthocyanins from *Gentiana lutea* L. var. *aurantiaca* petals by HPLC-ESI-MS/MS.**

| Peak number | Rt (min) | UV-maxima (nm) | Experimental [M] <sup>+</sup> ( <i>m/z</i> ) | Experimental MS/MS ( <i>m/z</i> )                 | Formula   | Assignment  | Petal Stage |
|-------------|----------|----------------|--|---|---|---|-------------|
| 1           | 6.88     | 274, 426, 498  | 741.22180                                    | 579.16992/433.11237/271.05966                     | C <sub>33</sub> H <sub>41</sub> O <sub>19</sub> | Pelargonidin 3- <i>O</i> -rutinoside-5- <i>O</i> -β-D-glucoside   | S3, S5      |
| 2           | 8.61     | 282, 497       | 595.16516                                    | 433.11273/271.05972                               | C <sub>27</sub> H <sub>31</sub> O <sub>15</sub> | Pelargonidin 3,5- <i>O</i> -diglucoside   | S1, S3, S5  |
| 3           | 11.15    | 498            | 579.17078                                    | 433.11307/271.05981/146.05790                     | C <sub>27</sub> H <sub>31</sub> O <sub>14</sub> | Pelargonidin 3- <i>O</i> -rutinoside  | S1, S3, S5  |
| 4           | 12.53    | 498            | 433.11203                                    | 271.05969   | C <sub>21</sub> H <sub>21</sub> O <sub>10</sub> | Pelargonidin 3- <i>O</i> -glucoside   | S1, S3, S5  |
| 5           | 12.73    | 282, 496       | 1094.29358                                   | 932.23883/771.21368/433.11273/271.06000           | C <sub>52</sub> H <sub>55</sub> O <sub>26</sub> | Pelargonidin 3- <i>O</i> -[2- <i>O</i> -(6-( <i>E</i> )-feruloyl-β-D-glucopyranosyl)-6- <i>O</i> -( <i>E</i> )-caffeoyl-β-D-glucopyranoside]-5- <i>O</i> -(β-D-glucopyranoside)             | S3, S5      |
| 6           | 13.07    | 447, 496       | 1079.30284                                   | 932.23871/771.21368/433.11273/271.05972           | C <sub>52</sub> H <sub>55</sub> O <sub>25</sub> | Pelargonidin 3- <i>O</i> -[2- <i>O</i> -(6-( <i>E</i> )-feruloyl-β-D-glucopyranosyl)-6- <i>O</i> -( <i>E</i> )- <i>p</i> -coumaroyl-β-D-glucopyranoside]-5- <i>O</i> -(β-D-glucopyranoside) | S3, S5      |
| 7           | 13.87    | 275,366, 500   | 843.22095                                    | 681.16675/595.16333/519.11456/433.11392/271.06033 | C <sub>39</sub> H <sub>39</sub> O <sub>21</sub> | Pelargonidin 3- <i>O</i> -(6- <i>O</i> -caffeoyl-D-glucoside)-5- <i>O</i> -(6- <i>O</i> -malonyl-β-D-glucoside)   | S3, S5      |
| 8           | 14.28    | 492            | 827.21936                                    | 579.17004/519.11230/271.05972                     | C <sub>36</sub> H <sub>43</sub> O <sub>22</sub> | Pelargonidin 3- <i>O</i> -(6- <i>p</i> -coumaroyl-D-glucoside)-5-(4- <i>O</i> -malonyl-β-D-glucoside)   | S3, S5      |
| 9           | 14.94    | 447, 496       | 681.16565                                    | 519.11298/433.11243/271.05963                     | C <sub>30</sub> H <sub>33</sub> O <sub>18</sub> | Pelargonidin 3- <i>O</i> -(6- <i>O</i> -malonyl-β-D-glucoside)-5-β-D-glucoside  | S3, S5      |
| 10          | 15.22    | 282, 496       | 517.09755                                    | 433.11307/271.06073                               | C <sub>24</sub> H <sub>21</sub> O <sub>13</sub> | Pelargonidin 3- <i>O</i> -(6- <i>O</i> -malonyl-β-D-glucoside)  | S1, S3, S5  |
| 11          | 15.66    | 447, 496       | 579.15012                                    | 433.11307/271.05957                               | C <sub>30</sub> H <sub>27</sub> O <sub>12</sub> | Pelargonidin 3- <i>O</i> -(6- <i>p</i> -coumaroyl)glucoside   | S1, S3, S5  |

<https://doi.org/10.1371/journal.pone.0212062.t001>

(A)



(B)

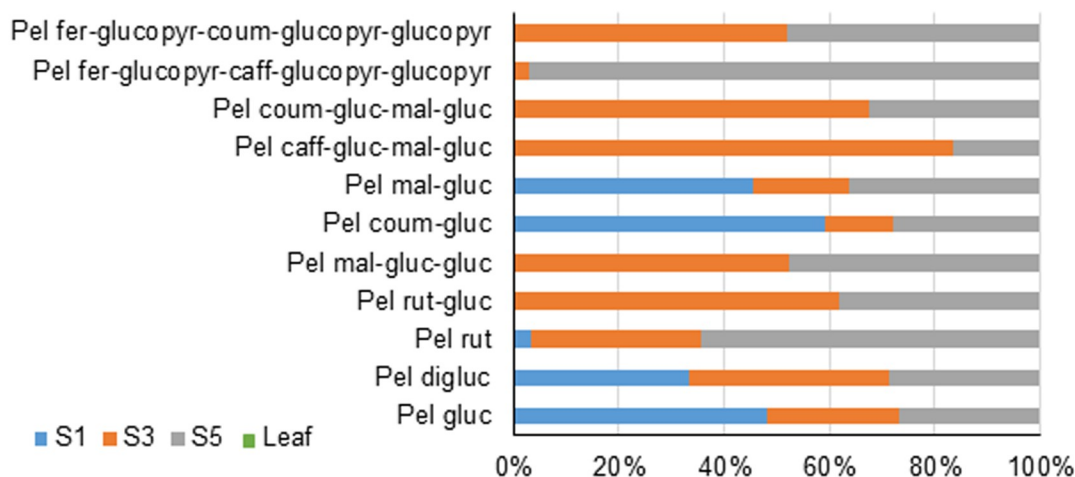


**Fig 3. Levels of pelargonidin derivatives identified in leaf and petals of *Gentiana lutea* L. var. *aurantiaca* in three different developmental stages by HPLC-ESI-MS/MS analyses.** (A) Data are expressed as average and standard deviation which represent, for each anthocyanin metabolite, the fold over the internal standard (IS), have been obtained by using, at least, 3 independent biological replicates. For more details, see [Materials and Methods](#). (B) Percent relative abundance of each anthocyanin among the three developmental stages (S1, S3, S5) under study. Abbreviations: Pel coum-gluc, Pelargonidin 3-O-(6-*p*-coumaroyl)glucoside; Pel digluc, Pelargonidin 3,5-O-diglucoside; Pel caff-gluc-mal-gluc, Pelargonidin 3-O-(6-*O*-caffeoyl-D-glucoside)-5-O-(6-*O*-malonyl-β-D-glucoside); Pel fer-glucopyr-caff-glucopyr-glucopyr, Pelargonidin 3-O-[2-O-(6-*E*)-feruloyl-β-D-glucopyranosyl]-6-*O*-(*E*)-caffeoyl-β-D-glucopyranoside]-5-O-(β-D-glucopyranoside); Pel fer-glucopyr-coum-glucopyr-glucopyr, Pelargonidin 3-O-[2-O-(6-*E*)-feruloyl-β-D-glucopyranosyl]-6-*O*-(*E*)-*p*-coumaroyl-β-D-glucopyranoside]-5-O-(β-D-glucopyranoside); Pel gluc, Pelargonidin 3-O-glucoside; Pel mal-gluc, Pelargonidin 3-O-(6-*O*-malonyl-β-D-glucoside); Pel rut, Pelargonidin 3-O-rutinoside; Pel rut-gluc, Pelargonidin 3-O-rutinoside-5-O-β-D-glucoside; Pel mal-gluc-gluc, Pelargonidin 3-O-(6-*O*-malonyl-β-D-glucoside)-5-β-D-glucoside; Pel coum-gluc-mal-gluc, Pelargonidin 3-O-(6-*p*-coumaroyl-D-glucoside)-5-(4-*O*-malonyl-β-D-glucoside).

<https://doi.org/10.1371/journal.pone.0212062.g003>

identified, albeit at very low amounts, were pelargonidin 3-*O*-rutinoside and pelargonidin 3-*O*-(6-*p*-coumaroyl)glucoside. Stage 3 (S3) displayed the presence of new pelargonidin derivatives not detected at S1, with four main derivatives: pelargonidin 3,5-*O*-diglucoside (33.4%),

pelargonidin 3-*O*-glucoside (32.5%), pelargonidin-3-*O*-(6-*p*-coumaroyl-*D*-glucoside)-5-(4-*O*-malonyl- $\beta$ -*D*-glucoside) (10.3%) and pelargonidin 3-*O*-rutinoside (9.6%) (Fig 3 and S2 Fig). Stage 5 (S5), corresponding to the flower in anthesis, showed the highest content in anthocyanins. In this tissue, the major derivatives of pelargonidin corresponded to pelargonidin 3-*O*-glucoside (34.5%), followed by pelargonidin 3,5-*O*-diglucoside (25.1%), pelargonidin 3-*O*-rutinoside (19.10%) and pelargonidin 3-*O*-(6-*O*-malonyl- $\beta$ -*D*-glucoside) (5.5%) (Fig 3). The formation of pelargonidin 3-*O*-glucoside, pelargonidin 5-*O*-glucoside, pelargonidin 3,5-*O*-diglucoside and pelargonidin 3-*O*-rutinoside are the most likely first steps of glycosylation in gentian petals (Fig 1), and are further modified by acylation reactions, leading to more diverse and complex pelargonidin molecules [41]. Notably, the anthocyanins molecules modified with aromatic acyl groups in their 3- and/or 5-positions appear to provide a reddish-purple color (without the interaction with co-pigments and/or metal ions) [41,42]. Overall, the biochemical analyses showed that there was a significant increase in pelargonidin glycosides as the petals developed, and such accumulation parallels the increasing orange coloration of the petals during development. In most plants, total anthocyanins content increases with the flower development and reaches its peak just before the buds open [43,44], with a rapid accumulation of anthocyanins in petals at the later stages of their development [45,46]. In order to better understand the relationships among the different anthocyanins detected, we performed a row-directed hierarchical clustering analysis (HCL) (S2 Fig). This analysis evidenced the presence of a main cluster placed in the top region and composed by pelargonidin 3-*O*-rutinoside and pelargonidin 3-*O*-glucoside, and some of their direct derivatives as pelargonidin 3-*O*-(6-*p*-coumaroyl)glucoside, pelargonidin 3-*O*-(6-*p*-coumaroyl-*D*-glucoside)-5-(4-*O*-malonyl- $\beta$ -*D*-glucoside), and pelargonidin 3-*O*-(6-*O*-malonyl- $\beta$ -*D*-glucoside), thus partially confirming the hypothesis that anthocyanins with simpler compositions as pelargonidin 3-*O*-glucoside acts as starting block for the production of more complex derivatives.

We further analyzed the levels of the flavonoid precursors in the anthocyanin pathway in the three developmental stages under study (Fig 4). Phenylalanine acts as the universal precursor of the phenylpropanoid pathway, leading to the production of coumarins, hydroxycinnamic acids, lignins, flavonoids, isoflavonoids, stilbenes, and of a wide variety of other phenolic compounds [6,7]. The levels of phenylalanine decreased from S1 to S3, and reached the maximum levels at S5 stage (Fig 4). Simultaneously, cinnamic acid displayed higher levels in stages S3 and S5, a pattern opposite to that of coumaric acid (Fig 4), which showed its highest content at S1 stage; finally late anthocyanins precursors like naringenin chalcone and naringenin gradually increased from S1 to S5 stages, while dihydrokaempferol was greatly reduced during flower development. The divergent trends of accumulation between a first metabolic group composed by cinnamic acid, naringenin chalcone and naringenin (increased levels from S1 to S5), and a second including coumaric acid and dihydrokaempferol (higher levels at S1, and lower at S3 and S5), could suggest the presence of a series of rate-limiting steps in gentian phenylpropanoid pathway, like in the case of cinnamic acid 4-hydroxylase (C4H) catalyzing aromatic ring-4 hydroxylation of cinnamic acid into *p*-coumaric acid, and/or flavonoid 3-hydroxylase (F3H) utilizing naringenin to yield dihydrokaempferol, which constrain pelargonidin accumulation in the petals during their development. In agreement with this hypothesis, PAL (phenylalanine ammonia-lyase) and C4H are part of a feedback loop controlling phenylpropanoid biosynthesis [47], which is acting at the entry point of the pathway; while F3H plays a role in regulating anthocyanin production in *Antirrhinum* [48].

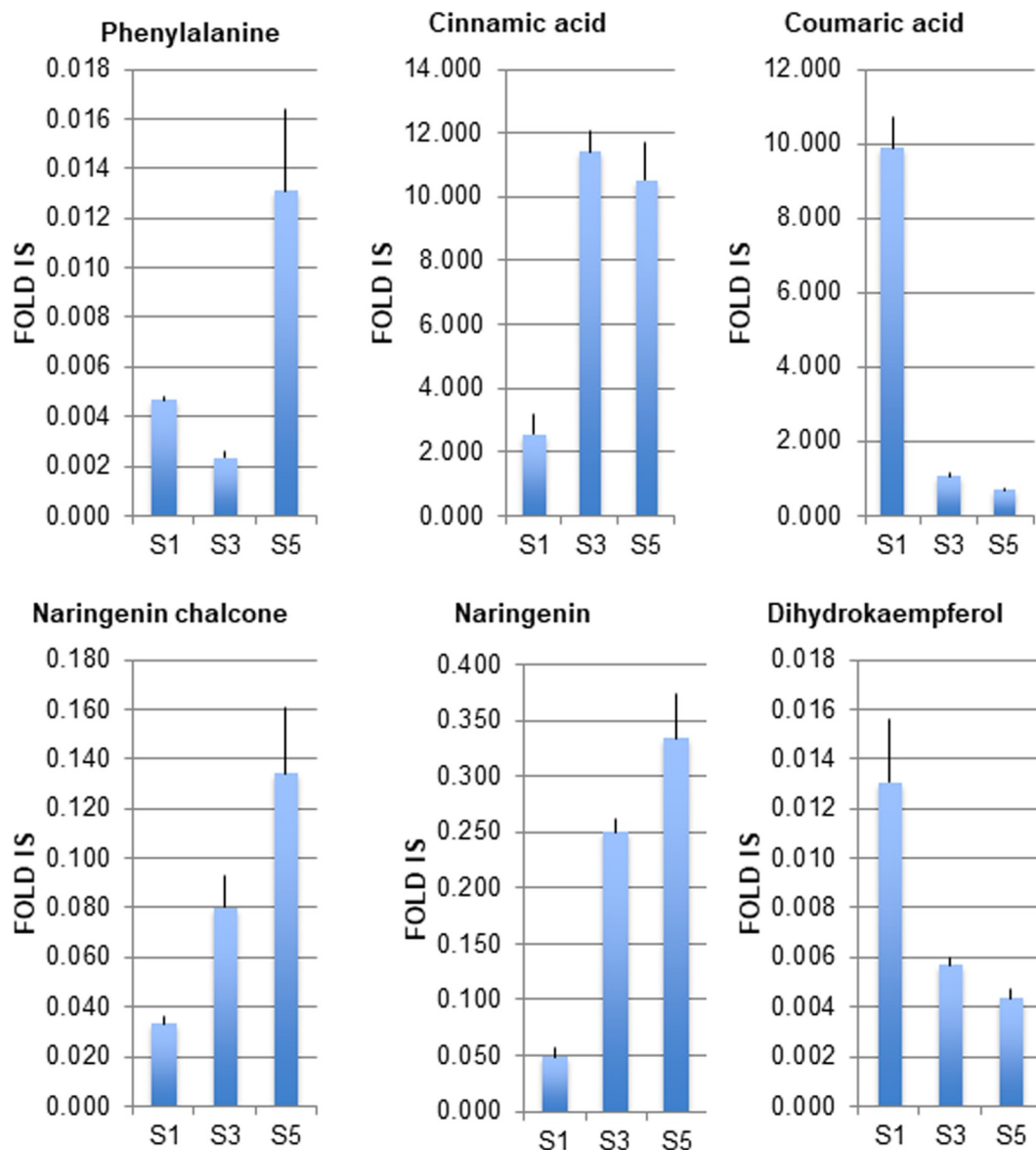


**Fig 4. Levels of anthocyanin precursors identified in petals of *Gentiana lutea* L. var. *aurantiaca* in three different developmental stages by HPLC-ESI-MS/MS analyses.** Data are expressed as average and standard deviation which represent, for each metabolite, the fold over the internal standard (IS), have been obtained by using, at least, three independent biological replicates. For more details, see [Materials and Methods](#).

<https://doi.org/10.1371/journal.pone.0212062.g004>

### Pelargonidin glucoside biosynthesis gene expression

As anthocyanin genes are mainly regulated at the level of transcription [49], we analyzed the expression levels of five key late anthocyanin biosynthesis genes (*DFR*, *ANS*, *3GT*, *5GT* and *5AT*) involved in the pelargonidin glycoside biosynthesis (Fig 1) in mature leaves and petals of *G. lutea* L. var. *aurantiaca* at S1, S3 and S5 stages. *DFR*, *ANS* and *3GT* genes were isolated in a recent study [21]. Furthermore, we cloned *5GT* and *5AT* gene fragments from mixed petals of stages S1, S3 and S5 by RT-PCR (see [Material and Methods](#)). Each PCR yielded a single product of the expected size. Cloning, sequencing and alignments of these cDNA fragments and their deduced encoding proteins (S3 and S4 Figs) demonstrated the isolated *5GT* and *5AT*



partial cDNAs had high identity (more than 88.0%, eliminating primer sequences) with those from *G. triflora* [10]. Quantitative RT-PCR (qRT-PCR) results of anthocyanin genes of interest are reported in Fig 5. The petals of *G. lutea* L. var. *aurantiaca* contained substantially higher levels of *DFR*, *ANS*, *3GT*, *5GT* and *5AT* mRNAs, while leaves displayed no accumulation of these mRNAs. In greater detail, higher relative levels of *DFR*, *ANS* and *3GT* mRNAs at stages S3 and S5 than at stage S1 were found, while similar levels of *5AT* mRNA at stages S1, S3 and S5 were observed (Fig 5). These findings are in agreement with previous studies, which showed relatively high expression levels of acyltransferase genes in the initial stages of petal development [50]. Notably, the levels of *5GT* mRNA at stage S1 were higher than at stages S3 and S5. A similar phenomenon has already been observed in carnation [51] and peony [52], where the gene encoding *5GT* is also expressed independently of other genes for anthocyanin biosynthesis [53].

### Integration of transcript and metabolite data of gentian phenylpropanoid pathway

To investigate more in the detail gentian anthocyanin biosynthesis, we calculated Pearson correlation coefficients ( $\rho$ s) for each data pair (transcript-transcript, transcript-metabolite, metabolite-metabolite), followed by correlation matrix and network visualizations (Fig 6A and 6B, respectively; see Materials and Methods). Overall, most of the correlations observed were of positive sign and very strong ( $\rho \geq 0.65$ ), indicating that most of transcript and metabolite levels are showing similar trends in their expression and accumulation. Thus, although at mathematical-based degree, this finding could suggest the presence of a high extent of coordination in the synthesis and the accumulation of pelargonidin anthocyanins along the flower petal development. However, a notable exception was found within *5GT* transcript (Fig 6A). The presence of a divergent altitude for this element could be associated to specific controls at gene expression or metabolite levels (rate limiting steps or negative feedback, as mentioned before). In addition, force-directed correlation network was exploited to highlight the most relevant elements in the dataset ("hubs" of the network) mainly responsible for the anthocyanin production and accumulation (Fig 6B). Interestingly, most of the pelargonidin anthocyanins placed, in a right- and top-side region in the network. Since, in a correlation network, the topology is generated by the correlations of the input file themselves, and nodes which do not display high number of significant correlations towards the rest of the nodes in the dataset normally localize in distal regions of the network, this evidence could provide clues about a non-active role in the control of the pathway. On the other hand, we found most of the genes located in the central area of the network. Among them, *DFR*, *ANS* and *3GT* were the ones displaying the highest number of very significant correlations, as evidenced by their topology as well by the node strength (ns) values (e.g. the average of all the  $|\rho|$ s yielded by each node) (S1 Table). Finally, the determination of a such high network strength (NS; equal to 0.76) obtained by through the calculation of all the  $|\rho|$ s in the network, could confirm the existence of strong and harmonic relationships both at transcript and metabolite level, underlying the generation of all the anthocyanin set in the petals of the orange gentian.

### Conclusions

Pelargonidin derivatives have been found in different plant species including orange cultivars of *Pelargonium* where they can account for up to 98% of total anthocyanins [54], *Dahlia variabilis* [55], magenta flowers of *Verbena* [56], red-purple flowers of *Matthiola incana* [57] and *Ipomoea purpurea* [58], red flowers of *Hyacinthus orientalis* [40], maroon flowers of *Pharbitis nil* [59], and white and pink flowers of *Muscari* spp. [44]. All identified anthocyanin molecules

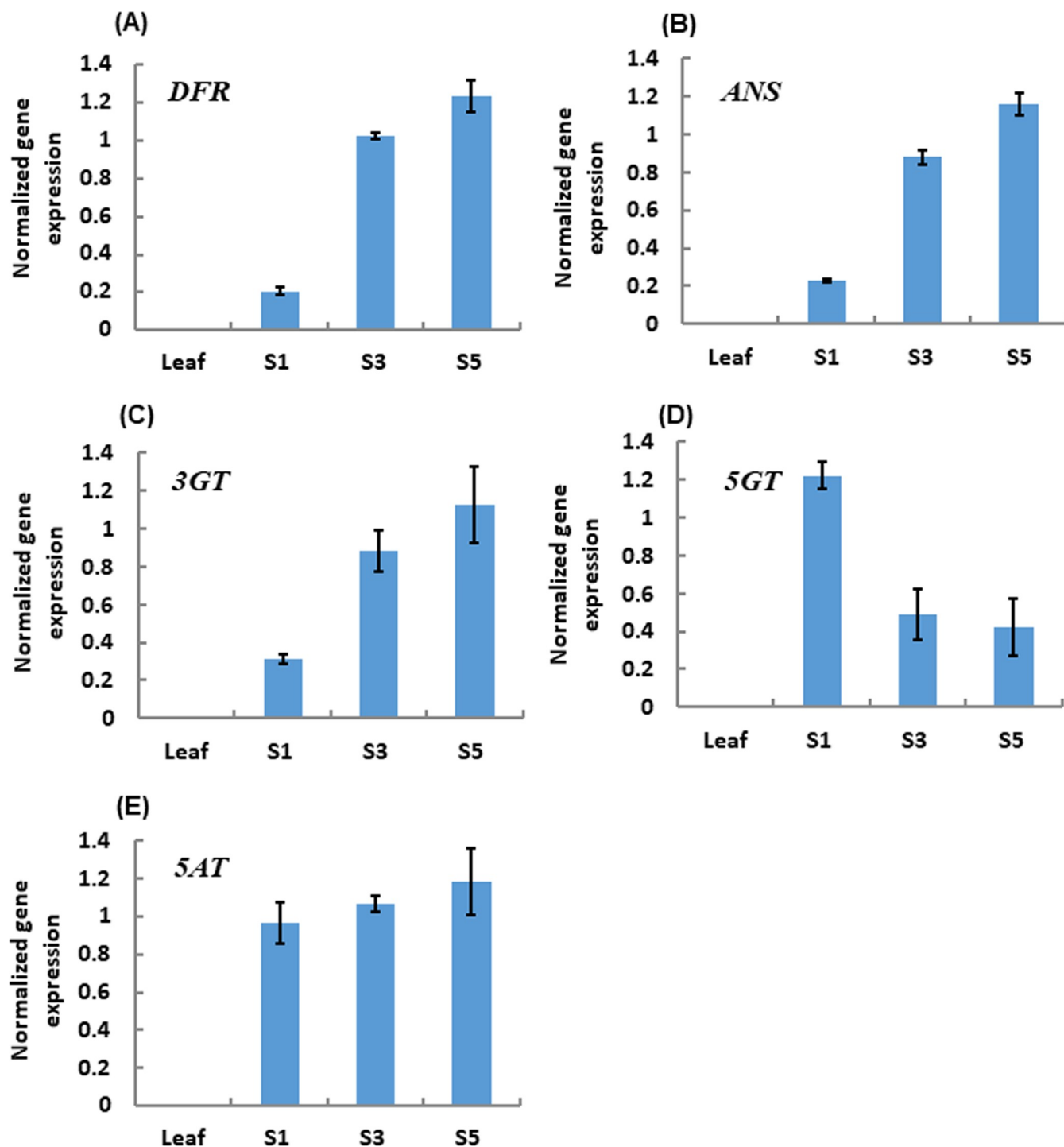


**Fig 5. Quantitative expression of anthocyanin genes, normalized on the ubiquitin housekeeping gene in leaf and petals of *Gentiana lutea* L. var. *aurantiaca*.** qRT-PCT data were calculated from three biological replicates with at least three technical replicates for each biological replicate and with error bars representing the standard deviation. Abbreviations: 5AT, anthocyanin 5-aromatic acyltransferase gene; ANS, anthocyanidin synthase gene; DFR, dihydroflavonol 4-reductase gene; 3GT, UDP-glucose:flavonoid 3-O-glucosyltransferase gene; 5GT, UDP-glucose:flavonoid 5-O-glucosyltransferase gene.

<https://doi.org/10.1371/journal.pone.0212062.g005>

of *G. lutea* L. var. *aurantiaca* were derived from side group modifications of pelargonidin, through different mechanisms of glycosylation and acylation. These modifications have been

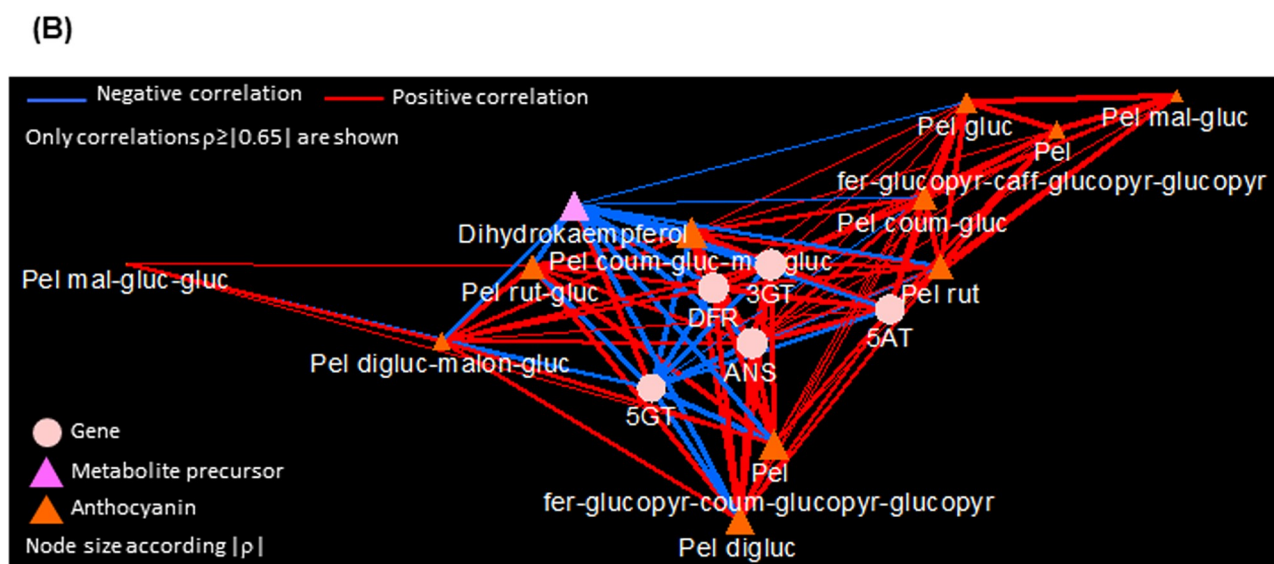
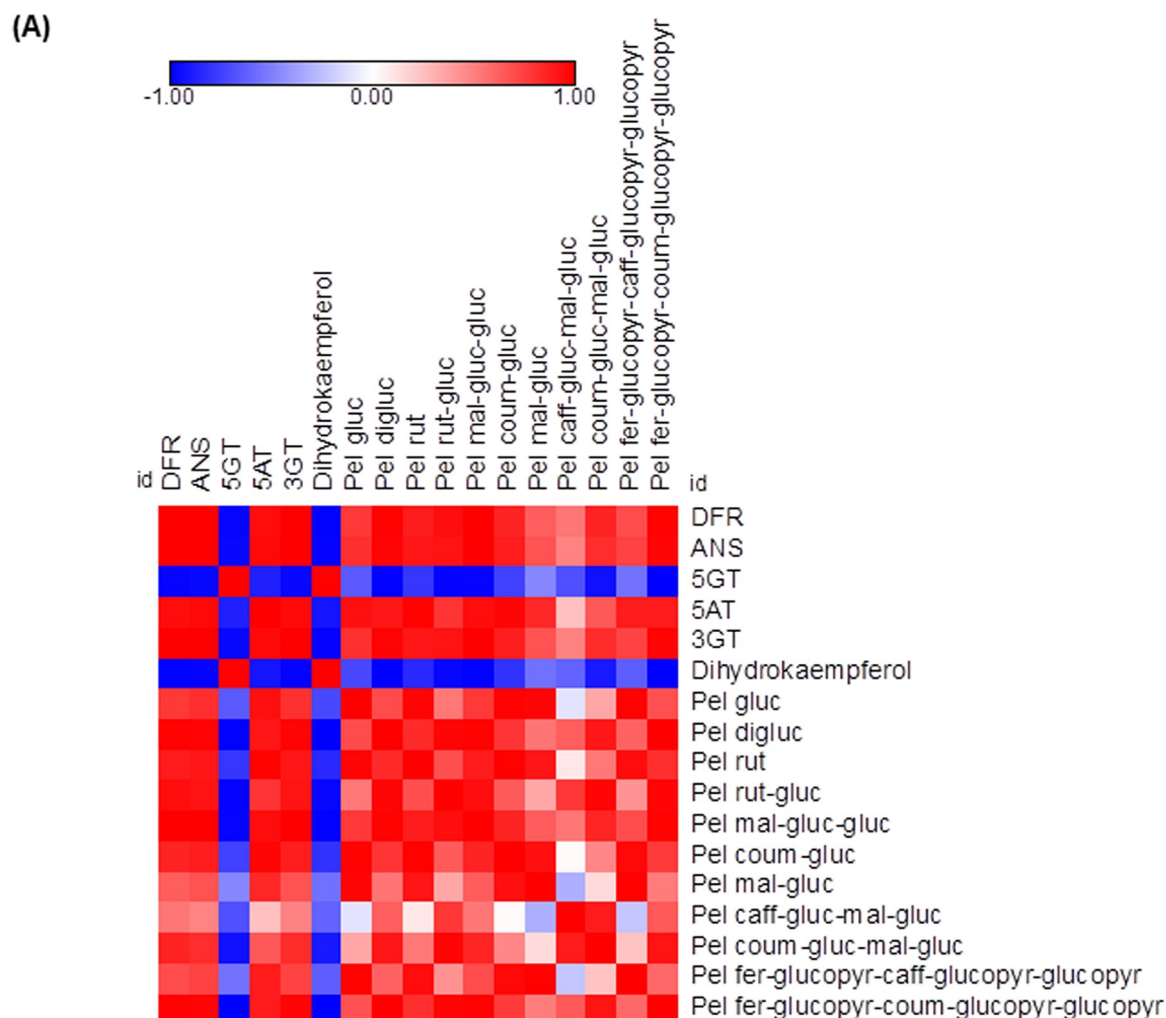


**Fig 6. Integration of transcript-metabolite data involved in *G. lutea* L. var. *aurantiaca* anthocyanin metabolism.** (A) Pearson coefficient-based correlation matrix. Legend on the right corresponds to the names of the anthocyanin transcripts and metabolites. Red and blue shaded boxes represent different levels of positive and negative correlations, respectively; white boxes represent no correlation. (B) Anthocyanin transcript/metabolite correlation network using a prefuse force-directed layout (only  $p > 0.65$  are shown). Transcripts, anthocyanins and anthocyanin precursors are represented, respectively, as pink rounds, and orange and violet triangles. Blue and red edges refer to negative and positive correlations, respectively. Node size is according to the node strength (ns, representing the average of all the ps of each node). Lines joining the nodes indicate positive (red) and negative (blue) correlations, of width proportional to each corresponding  $|p|$ . Abbreviations: ANS, anthocyanidin synthase; 5AT, anthocyanin 5-aromatic acyltransferase; DFR, dihydroflavonol 4-reductase; 3GT, UDP-glucose:flavonoid 3-O-glucosyltransferase gene; 5GT, UDP-glucose:flavonoid 5-O-glucosyltransferase; Pel coum-gluc, Pelargonidin 3-O-(6-*p*-coumaroyl)glucoside; Pel digluc, Pelargonidin 3,5-O-diglucoside; Pel caff-gluc-mal-gluc, Pelargonidin 3-O-(6-O-caffeoyl-D-glucoside)-5-O-(6-O-malonyl-β-D-glucoside); Pel fer-glucopyr-caff-glucopyr-glucopyr, Pelargonidin 3-O-[2-O-(6-(E)-feruloyl-β-D-glucopyranosyl)-6-O-(E)-caffeoyl-β-D-glucopyranoside]-5-O-(β-D-glucopyranoside); Pel fer-glucopyr-coum-glucopyr-glucopyr, Pelargonidin 3-O-[2-O-(6-(E)-feruloyl-β-D-glucopyranosyl)-6-O-(E)-*p*-coumaroyl-β-D-glucopyranoside]-5-O-(β-D-glucopyranoside); Pel gluc, Pelargonidin 3-O-glucoside; Pel mal-gluc, Pelargonidin 3-O-(6-O-malonyl-β-D-glucoside); Pel rut, Pelargonidin 3-O-rutinoside; Pel rut-gluc, Pelargonidin 3-O-rutinoside-5-O-β-D-glucoside; Pel mal-gluc-gluc, Pelargonidin 3-O-(6-O-malonyl-β-D-glucoside)-5-β-D-glucoside; Pel coum-gluc-mal-gluc, Pelargonidin 3-O-(6-*p*-coumaroyl-D-glucoside)-5-(4-O-malonyl-β-D-glucoside).

<https://doi.org/10.1371/journal.pone.0212062.g006>

reported to increase anthocyanin stability in aqueous solution and may likely alter their light absorption properties [6,60]. All metabolites identified contained at least one sugar group. The hydroxyl groups at C<sub>3</sub> and C<sub>5</sub> positions of pelargonidin have been reported to be the two commonest targets of glucosylation [60]. In the present study, we revealed that pelargonidin 3-O-glucoside, pelargonidin 3,5-O-diglucoside and pelargonidin 3-O-rutinoside are the main pelargonidin derivatives present in *G. lutea* L. var. *aurantiaca* petals. However, besides the presence of these molecules, other more complex pelargonidin derivatives were tentatively identified. We analyzed the expression of late *DFR*, *ANS*, *3GT*, *5GT* and *5AT* genes specifically for anthocyanin biosynthesis in the petals of *G. lutea* L. var. *aurantiaca* to determine the molecular mechanisms responsible for the accumulation of pelargonidin glycosides during flower development. The accumulation of the pelargonidin glucosides parallels the expression levels of the genes *DFR*, *ANS* and *3GT*, suggesting their main role in the accumulation of these anthocyanins in *G. lutea* L. var. *aurantiaca* flowers, with *DFR* most probably acting as the limiting step in this process [21]. The resulting data will enhance our understanding of the structural diversity of anthocyanin molecules in *Gentiana* species, and lays a foundation for breeding of flower color and genetic variation studies on *Gentiana* varieties.

## Supporting information

**S1 Fig. HPLC-PDA chromatographic profiles of the anthocyanins in *Gentiana lutea* L. var. *aurantiaca* petals at the S5 stage.** A, HPLC-DAD/UV isoplot from 200–600 nm. Anthocyanins are detected in the 500 nm range. B and C, correspond to magnifications in the 500 nm range to show up the anthocyanins present in lower amounts. D, HPLC-DAD chromatogram at 505 nm, showing the profile of the anthocyanins present in the S5 extract. (PDF)

**S2 Fig. Row-directed Hierarchical clustering (HCL) visualization of anthocyanin metabolites detected in petals of *G. lutea* L. var. *aurantiaca*.** Data represent, for each metabolite, the fold over the internal standard (IS) intensity. Abbreviations: Pel coum-gluc, Pelargonidin 3-O-(6-*p*-coumaroyl)glucoside; Pel digluc, Pelargonidin 3,5-O-diglucoside; Pel caff-gluc-mal-gluc, Pelargonidin 3-O-(6-O-caffeoyl-D-glucoside)-5-O-(6-O-malonyl-β-D-glucoside); Pel fer-glucopyr-caff-glucopyr-glucopyr, Pelargonidin 3-O-[2-O-(6-(E)-feruloyl-β-D-glucopyranosyl)-6-O-(E)-caffeoyl-β-D-glucopyranoside]-5-O-(β-D-glucopyranoside); Pel fer-glucopyr-coum-glucopyr-glucopyr, Pelargonidin 3-O-[2-O-(6-(E)-feruloyl-β-D-glucopyranosyl)-6-O-(E)-*p*-coumaroyl-β-D-glucopyranoside]-5-O-(β-D-glucopyranoside); Pel gluc, Pelargonidin 3-O-glucoside; Pel mal-gluc, Pelargonidin 3-O-(6-O-malonyl-β-D-glucoside); Pel rut, Pelargonidin 3-O-rutinoside; Pel rut-gluc, Pelargonidin 3-O-rutinoside-5-O-β-D-glucoside; Pel mal-gluc-

gluc, Pelargonidin 3-O-(6-O-malonyl- $\beta$ -D-glucoside)-5- $\beta$ -D-glucoside; Pel coum-gluc-mal-gluc, Pelargonidin 3-O-(6-*p*-coumaroyl-D-glucoside)-5-(4-O-malonyl- $\beta$ -D-glucoside). (PDF)

**S3 Fig. Alignments of partial 5GT and 5AT cDNA sequences encoding UDP-glucose:flavonoid 5-O-glucosyltransferase (5GT; A) and anthocyanin 5-aromatic acyltransferase (5AT; B) between *Gentiana triflora* (Gt) and *G. lutea* L. var. *aurantiaca* (Gla).** The underlined cDNA sequences indicate the primers used to isolate cDNA fragments from petals of *G. lutea* L. var. *aurantiaca*. Gaps are inserted with a dash (-) in one of the sequences. Abbreviations: Gt, *Gentiana triflora*; Gla, *G. lutea* L. var. *aurantiaca*; 5GT, UDP-glucose:flavonoid 5-O-glucosyltransferase gene; 5AT, anthocyanin 5-aromatic acyltransferase gene. GenBank accession numbers: Gt5GT, AB363839; Gt5AT, AB010708. The partial cDNA sequences of 5GT and 5AT genes from *G. lutea* L. var. *aurantiaca* have been isolated by the authors in this study. (PDF)

**S4 Fig. Alignments of the deduced amino acid sequences encoded by UDP-glucose:flavonoid 5-O-glucosyltransferase (5GT) gene (A), and anthocyanin 5-aromatic acyltransferase (5AT) gene (B) from *Gentiana triflora* and *G. lutea* L. var. *aurantiaca*.** Gaps are inserted with a dash (-) in one of the sequences. The underlined amino acid sequences from *G. lutea* L. var. *aurantiaca* were deduced from primers. Abbreviations: Gt, *Gentiana triflora*; Gla, *G. lutea* L. var. *aurantiaca*; 5GT, UDP-glucose:flavonoid 5-O-glucosyltransferase; 5AT, anthocyanin 5-aromatic acyltransferase. GenBank accession numbers: Gt5GT, AB363839; Gt5AT, AB010708. The partial amino acid sequences of 5GT and 5AT of *G. lutea* L. var. *aurantiaca* were deduced from partial cDNA sequences cloned by the authors in this study. (PDF)

**S1 Table. Node strength (ns) and network strength (NS) of gentian phenylpropanoid genes and metabolites, expressed as the average of all the |ps| yielded by a node and the average of the ns, respectively.** (PDF)

## Acknowledgments

We thank Drs Tania Veiga, Javier Guitián and Pablo Guitián of Departamento de Botánica, Universidad de Santiago de Compostela, Galicia, Spain for supplying the orange-flowered gentian (*G. lutea* L. var. *aurantiaca*) flowers.

## Author Contributions

**Conceptualization:** Changfu Zhu, Lourdes Gomez-Gomez.

**Formal analysis:** Gianfranco Diretto, Xin Jin, Teresa Capell, Changfu Zhu, Lourdes Gomez-Gomez.

**Investigation:** Gianfranco Diretto, Xin Jin, Teresa Capell, Changfu Zhu, Lourdes Gomez-Gomez.

**Methodology:** Gianfranco Diretto, Xin Jin, Teresa Capell, Lourdes Gomez-Gomez.

**Project administration:** Gianfranco Diretto, Xin Jin, Teresa Capell, Changfu Zhu, Lourdes Gomez-Gomez.

**Supervision:** Changfu Zhu.

**Validation:** Xin Jin.



**Writing – original draft:** Gianfranco Diretto, Xin Jin, Changfu Zhu, Lourdes Gomez-Gomez.

**Writing – review & editing:** Changfu Zhu, Lourdes Gomez-Gomez.

## References

1. Fenster CB, Armbruster WS, Wilson P, Dudash MR, Thomson JD. Pollination syndromes and floral specialization. *Annu Rev Ecol Evol Syst.* 2004; 35:375–403.
2. Harborne JB. Spectral methods of characterizing anthocyanins. *Biochem J.* 1958; 70: 22–28. PMID: [13584295](#)
3. Harborne JB. Anthocyanins and their sugar components. *Fortschr Chem Org Naturst.* 1962; 20: 165–199. PMID: [13952723](#)
4. Tanaka Y, Sasaki N, Ohmiya A. Biosynthesis of plant pigments: anthocyanins, betalains and carotenoids. *Plant J.* 2008; 54: 733–749. <https://doi.org/10.1111/j.1365-313X.2008.03447.x> PMID: [18476875](#)
5. Tanaka Y, Ohmiya A. Seeing is believing: engineering anthocyanin and carotenoid biosynthetic pathways. *Curr Opin Biotechnol.* 2008; 19: 190–197. <https://doi.org/10.1016/j.copbio.2008.02.015> PMID: [18406131](#)
6. Shi MZ, Xie DY. Biosynthesis and metabolic engineering of anthocyanins in *Arabidopsis thaliana*. *Recent Pat Biotechnol.* 2014; 8: 47–60. <https://doi.org/10.2174/1872208307666131218123538> PMID: [24354533](#)
7. Zhang Y, Butelli E, Martin C. Engineering anthocyanin biosynthesis in plants. *Curr Opin Plant Biol.* 2014; 19: 81–90. <https://doi.org/10.1016/j.pbi.2014.05.011> PMID: [24907528](#)
8. Holton TA. Modification of flower colour via manipulation of P450 gene expression in transgenic plants. *Drug Metabol Drug Interact.* 1995; 12: 359–368. PMID: [8820861](#)
9. Kamsteeg J, van Brederode J, van Nigtevecht G. Identification, properties, and genetic control of UDP-glucose: cyanidin-3-rhamnosyl-(1 leads to 6)-glucoside-5-O-glucosyltransferase isolated from petals of the red campion (*Silene dioica*). *Biochem Genet.* 1978; 16: 1059–1071. PMID: [751641](#)
10. Nakatsuka T, Sato K, Takahashi H, Yamamura S, Nishihara M. Cloning and characterization of the UDP-glucose:anthocyanin 5-O-glucosyltransferase gene from blue-flowered gentian. *J Exp Bot.* 2008; 59: 1241–1252. <https://doi.org/10.1093/jxb/ern031> PMID: [18375606](#)
11. Giusti MM, Wrolstad RE. Acylated anthocyanins from edible sources and their applications in food systems. *Biochem Eng J.* 2003; 14: 217–225.
12. Fujiwara H, Tanaka Y, Fukui Y, Nakao M, Ashikari T, Kusumi T. Anthocyanin 5-aromatic acyltransferase from *Gentiana triflora*. Purification, characterization and its role in anthocyanin biosynthesis. *Eur J Biochem.* 1997; 249: 45–51. PMID: [9363752](#)
13. Kohlein F. *Gentians*. Portland, Oregon, USA: Timber Press Inc.; 1991, pp. 25–27.
14. Fukuchi-Mizutani M, Okuhara H, Fukui Y, Nakao M, Katsumoto Y, Yonekura-Sakakibara K, et al. Biochemical and molecular characterization of a novel UDP-glucose:anthocyanin 3'-O-glucosyltransferase, a key enzyme for blue anthocyanin biosynthesis, from gentian. *Plant Physiol.* 2003; 132: 1652–1663. <https://doi.org/10.1104/pp.102.018242> PMID: [12857844](#)
15. Yoshida K, Mori M, Kondo T. Blue flower color development by anthocyanins: from chemical structure to cell physiology. *Nat Prod Rep.* 2009; 26: 884–915. <https://doi.org/10.1039/b800165k> PMID: [19554240](#)
16. Hosokawa K, Fukushi E, Kawabata J, Fuji C, Ito T, Yamamura S. Three acylated cyanidin glucosides in pink flowers of *Gentiana*. *Phytochem.* 1995; 40: 941–944.
17. Nakatsuka T, Nishihara M, Mishiba K, Yamamura S. Two different mutations are involved in the formation of white-flowered gentian plants. *Plant Sci.* 2005; 169: 949–958.
18. Nakatsuka T, Nishihara M, Mishiba K, Hirano H, Yamamura S. Two different transposable elements inserted in flavonoid 3',5'-hydroxylase gene contribute to pink flower coloration in *Gentiana scabra*. *Mol Genet Genomics.* 2006; 275: 231–241. <https://doi.org/10.1007/s00438-005-0083-7> PMID: [16362368](#)
19. Mu J, Yang Y, Luo Y, Su R, Niklas KJ. Pollinator preference and pollen viability mediated by flower color synergistically determine seed set in an Alpine annual herb. *Ecol Evol.* 2017; 7: 2947–2955. <https://doi.org/10.1002/ece3.2899> PMID: [28479994](#)
20. Renobales G. Notas acerca del tratamiento de las gentianaceae para flora ibérica. *Anales del Jardín Botánico de Madrid.* 2003; 60: 461–469.

21. Berman J, Sheng Y, Gomez-Gomez L, Veiga T, Ni X, Farre G, et al. Red anthocyanins and yellow carotenoids form the color of orange-flower gentian (*Gentiana lutea* L. var. *aurantiaca*). PLoS One. 2016; 11: e0162410. <https://doi.org/10.1371/journal.pone.0162410> PMID: 27589396
22. Harborne JB, Sherratt HS. Variations in the glycosidic pattern of anthocyanins. II. Experientia. 1957; 13: 486–487. PMID: 13512285
23. Harborne JB, Williams CA. Anthocyanins and other flavonoids. Nat Prod Rep. 2001; 18: 310–333. PMID: 11476484
24. Hong V, Wrolstad RE. Use of HPLC separation photodiode array detection for characterization of anthocyanins. J Agric Food Chem. 1990; 38: 707–715.
25. Sun J, Lin LZ, Chen P. Study of the mass spectrometric behaviors of anthocyanins in negative ionization mode and its applications for characterization of anthocyanins and non-anthocyanin polyphenols. Rapid Commun Mass Spectrom. 2012; 26: 1123–1133. <https://doi.org/10.1002/rcm.6209> PMID: 22467463
26. Wu X, Prior RL. Systematic identification and characterization of anthocyanins by HPLC-ESI-MS/MS in common foods in the United States: fruits and berries. J Agric Food Chem. 2005; 53: 2589–2599. <https://doi.org/10.1021/jf048068b> PMID: 15796599
27. Rambla JL, Trapero-Mozos A, Diretto G, Rubio-Moraga A, Granell A, Gomez-Gomez L, et al. Gene-Metabolite Networks of Volatile metabolism in airen and tempranillo grape cultivars revealed a distinct mechanism of aroma bouquet production. Front Plant Sci. 2016; 7: 1619. <https://doi.org/10.3389/fpls.2016.01619> PMID: 27833635
28. Maloney GS, DiNapoli KT, Muday GK. The anthocyanin reduced tomato mutant demonstrates the role of flavonols in tomato lateral root and root hair development. Plant Physiol. 2014; 166: 614–631. <https://doi.org/10.1104/pp.114.240507> PMID: 25006027
29. Ahrazem O, Argandona J, Fiore A, Aguado C, Lujan R, Rubio-Moraga A, et al. Transcriptome analysis in tissue sectors with contrasting crocins accumulation provides novel insights into apocarotenoid biosynthesis and regulation during chromoplast biogenesis. Sci Rep. 2018; 8: 2843. <https://doi.org/10.1038/s41598-018-21225-z> PMID: 29434251
30. Gomez-Gomez L, Parra-Vega V, Rivas-Sendra A, Segui-Simarro JM, Molina RV, Pallotti C, et al. Unraveling massive crocins transport and accumulation through proteome and microscopy tools during the development of saffron stigma. Int J Mol Sci. 2017; 18: pii: E76. <https://doi.org/10.3390/ijms18010076> PMID: 28045431
31. Diretto G, Al-Babili S, Tavazza R, Scossa F, Papacchioli V, Migliore M, et al. Transcriptional-metabolic networks in beta-carotene-enriched potato tubers: the long and winding road to the Golden phenotype. Plant Physiol. 2010; 154: 899–912. <https://doi.org/10.1104/pp.110.159368> PMID: 20671108
32. Sulli M, Mandolino G, Sturaro M, Onofri C, Diretto G, Parisi B, et al. Molecular and biochemical characterization of a potato collection with contrasting tuber carotenoid content. PLoS One. 2017; 12: e0184143. <https://doi.org/10.1371/journal.pone.0184143> PMID: 28898255
33. Kim HW, Kim JB, Cho SM, Chung MN, Lee YM, Chu SM, et al. Anthocyanin changes in the Korean purple-fleshed sweet potato, Shinzami, as affected by steaming and baking. Food Chem. 2012; 130: 966–972.
34. Koshioka M, Umegaki N, Boontiang K, Pornchuti W, Thammasiri K, Yamaguchi S, et al. Anthocyanins in the bracts of *Curcuma* species and relationship of the species based on anthocyanin composition. Nat Prod Commun. 2015; 10: 453–456. PMID: 25924528
35. Shim YS, Yoon WJ, Kim DM, Watanabe M, Park HC, Jang HW, et al. The simple determination method for anthocyanidin aglycones in fruits using ultra-high-performance liquid chromatography. J Chromatogr Sci. 2015; 53: 1646–1653. <https://doi.org/10.1093/chromsci/bmv064> PMID: 26041248
36. Yildirim S, Kadioglu A, Saglam A, Yasar A, Sellitepe HE. Fast determination of anthocyanins and free pelargonidin in fruits, fruit juices, and fruit wines by high-performance liquid chromatography using a core-shell column. J Sep Sci. 2016; 39: 3927–3935. <https://doi.org/10.1002/jssc.201600661> PMID: 27550473
37. Harborne JB. The chromatographic identification of anthocyanin pigments. J Chromatogr. 1958; 1: 210–224.
38. Rodriguez-Saona LE, Giusti MM, Wrolstad RE. Anthocyanin pigment composition of red-fleshed potatoes. J Food Sci. 1998; 63: 458–465.
39. Barnes JS, Schug KA. Structural characterization of cyanidin-3,5-diglucoside and pelargonidin-3,5-diglucoside anthocyanins: Multi-dimensional fragmentation pathways using high performance liquid chromatography-electrospray ionization-ion trap-time of flight mass spectrometry. Int J Mass Spectrom. 2011; 308: 71–80.

40. Hosokawa K, Fukunaga Y, Fukushi E, Kawabata J. Seven acylated anthocyanins in the blue flowers of *Hyacinthus orientalis*. *Phytochem*. 1995; 38: 1293–1298.
41. Sasaki N, Nishizaki Y, Ozeki Y, Miyahara T. The role of acyl-glucose in anthocyanin modifications. *Molecules*. 2014; 19: 18747–18766. <https://doi.org/10.3390/molecules191118747> PMID: 25405291
42. Sasaki N, Nakayama T. Achievements and perspectives in biochemistry concerning anthocyanin modification for blue flower coloration. *Plant Cell Physiol*. 2015; 56: 28–40. <https://doi.org/10.1093/pcp/pcu097> PMID: 25015943
43. Justesen H, Andersen AS, Brandt K. Accumulation of anthocyanins and flavones during bud and flower development in *Campanula isophylla* Moretti. *Ann Bot*. 1997; 79: 355–360.
44. Lou Q, Wang L, Liu H, Liu Y. Anthocyanin profiles in flowers of *Grape hyacinth*. *Molecules*. 2017; 22. pii: E688. <https://doi.org/10.3390/molecules22050688> PMID: 28445423
45. Lai YS, Shimoyamada Y, Nakayama M, Yamagishi M. Pigment accumulation and transcription of LhMYB12 and anthocyanin biosynthesis genes during flower development in the Asiatic hybrid lily (*Lilium* spp.). *Plant Sci*. 2012; 193–194: 136–147. <https://doi.org/10.1016/j.plantsci.2012.05.013> PMID: 22794927
46. Yamagishi M, Shimoyamada Y, Nakatsuka T, Masuda K. Two *R2R3-MYB* genes, homologs of *Petunia AN2*, regulate anthocyanin biosyntheses in flower Tepals, tepal spots and leaves of asiatic hybrid lily. *Plant Cell Physiol*. 2010; 51: 463–474. <https://doi.org/10.1093/pcp/pcq011> PMID: 20118109
47. Blount JW, Korth KL, Masoud SA, Rasmussen S, Lamb C, Dixon RA. Altering expression of cinnamic acid 4-hydroxylase in transgenic plants provides evidence for a feedback loop at the entry point into the phenylpropanoid pathway. *Plant Physiol*. 2000; 122: 107–116. PMID: 10631254
48. Martin C, Gerats T. Control of pigment biosynthesis genes during petal development. *Plant Cell*. 1993; 5: 1253–1264. <https://doi.org/10.1105/tpc.5.10.1253> PMID: 12271025
49. Nakatsuka T, Nishihara M, Mishiba K, Yamamura S. Temporal expression of flavonoid biosynthesis-related genes regulates flower pigmentation in gentian plants. *Plant Sci*. 2005; 168: 1309–1318.
50. Fujiwara H, Tanaka Y, Yonekura-Sakakibara K, Fukuchi-Mizutani M, Nakao M, Fukui Y, et al. cDNA cloning, gene expression and subcellular localization of anthocyanin 5-aromatic acyltransferase from *Gentiana triflora*. *Plant J*. 1998; 16: 421–431. PMID: 9881162
51. Matsuba Y, Sasaki N, Tera M, Okamura M, Abe Y, Okamoto E, et al. A novel glucosylation reaction on anthocyanins catalyzed by acyl-glucose-dependent glucosyltransferase in the petals of carnation and delphinium. *Plant Cell*. 2010; 22: 3374–3389. <https://doi.org/10.1105/tpc.110.077487> PMID: 20971893
52. Zhao D, Jiang Y, Ning C, Meng J, Lin S, Ding W, et al. Transcriptome sequencing of a chimaera reveals coordinated expression of anthocyanin biosynthetic genes mediating yellow formation in herbaceous peony (*Paeonia lactiflora* Pall.). *BMC Genomics*. 2014; 15: 689. <https://doi.org/10.1186/1471-2164-15-689> PMID: 25134523
53. Yabuya T, Yamaguchi M, Imayama T, Katoh K, Ino I. Anthocyanin 5-O-glucosyltransferase in flowers of *Iris ensata*. *Plant Sci*. 2002; 162: 779–784.
54. Mitchell KA, Markhama KR, Boase MR. Pigment chemistry and colour of *Pelargonium* flowers. *Phytochem*. 1998; 47: 355–361.
55. Ohno S, Hosokawa M, Hoshino A, Kitamura Y, Morita Y, Park KI, et al. A bHLH transcription factor, DvIVS, is involved in regulation of anthocyanin synthesis in dahlia (*Dahlia variabilis*). *J Exp Bot*. 2011; 62: 5105–5116. <https://doi.org/10.1093/jxb/err216> PMID: 21765172
56. Toki K, Saito N, Terahara N, Honda T. Pelargonidin 3-glucoside-5-acetylglucoside in *Verbena* flowers. *Phytochem*. 1995; 40: 939–940.
57. Saito N, Tatsuzawa F, Hongo A, Win KW, Yokoi M, Shigihara A, et al. Acylated pelargonidin 3-sambubioside-5-glucosides in *Matthiola incana*. *Phytochem*. 1996; 41: 1613–1620.
58. Saito N, Tatsuzawa F, Yokoi M, Kasahara K, Iida S, Shigihara A, et al. Acylated pelargonidin glycosides in red-purple flowers of *Ipomoea purpurea*. *Phytochem*. 1996; 43: 1365–1370.
59. Lu TS, Saito N, Yokoi M, Shigihara A, Honda T. Acylated pelargonidin glycosides in the red-purple flowers of *Pharbitis nil*. *Phytochem*. 1992; 31: 289–295.
60. Yonekura-Sakakibara K, Nakayama T, Yamazaki M, Saito K. Modification and stabilization of anthocyanins. In: Gould K, Davies K, Winefield C, editors. *Anthocyanins: Biosynthesis, functions and applications*. New York; Springer 2009: pp. 169–185.